ISSN: 2414-1895 DOI: 10.6919/ICJE.202404_10(4).0012

Conveyor Belt Buckle Groove Stamping Forming and Parameter Optimization

Jianglin Song, Zezhong Chen*, and Yun Meng

School of Materials and Chemistry, University of Shanghai for Science and Technology, Shanghai 200093, China

*961068964@qq.com

Abstract

The stamping numerical simulation of 304 stainless steel conveyor belt buckle groove was performed by ABAQUS finite element simulation software. The stamping process was simulated with various process parameters, including different friction coefficient, stamping speed, groove depth and mold fillet radii. The maximum thinning rate can serve as an indicator. Orthogonal tests were conducted on key parameters to optimize the stamping process parameters. Optimal process parameters were found to be 0.10 friction coefficient, 3200 mm/s punching speed, 3.7 mm groove depth, and 0.8 mm mold fillet radius.

Keywords

Stamping & Forming; CAE; Stamping Speed; Friction Coefficient; Depth of Groove.

1. Introduction

China is the leading coal-producing country and has the world's largest underground conveyor belt usage. With the rapid development of industrial production, coal demand has increased, but coal mining risk has also increased, and public safety has become a major concern. During conveyor belt operation, any breakage can easily lead to production safety accidents[1].

The quality of the conveyor belt splice has a direct impact on the life and operation of the conveyor belt, as all types of conveyor belts currently available on the market must be spliced into a ring in order to be used[2]. There are three types of conveyor belt splicing processes: mechanical splicing, cold adhesive splicing and hot vulcanized splicing. Among them, the mechanical splicing process is widely used because of its advantages of convenient production and fast operation. This method mainly connects the belt using mechanical belt buckles.

304 stainless steel is an austenitic stainless steel. It is widely used in various industries[3]. Due to its excellent abrasion resistance, corrosion resistance, and anti-magnetic properties, 304 stainless steel retains good strength even under conditions of high temperature and complex electromagnetic interference[4]. Stamping and forming is a process that combines elastic and plastic deformation. A press is used to apply pressure to the punch-pin. This causes the punch-pin to move and produces plastic deformation or separation of the material being processed[5]. After machining, the material is plastically deformed and takes a specific shape.

The stamping numerical simulation of 304 stainless steel conveyor belt buckle groove was performed by ABAQUS finite element simulation software. The stamping process was simulated with various process parameters, including different friction coefficient, stamping speed, groove depth and mold fillet radii. The maximum thinning rate can serve as an indicator. Stamping process parameters are optimized by orthogonal testing of key parameters using maximum thinning rate as an index, providing guidance for actual processing[6].

ISSN: 2414-1895 DOI: 10.6919/ICJE.202404_10(4).0012

2. Parameter Settings for Finite Element Modeling and Simulation

2.1 Creation of Geometric Model

The plate with the dimensions 125 mm x 21 mm x 2 mm was modeled in ABAQUS using shell unit. Model the punch-pin and cavity mold shapes in SolidWorks as shown in Figure 1. The dimensions of the punch-pin and cavity mold shapes are shown in Figure 1. They are saved and imported into ABAQUS.

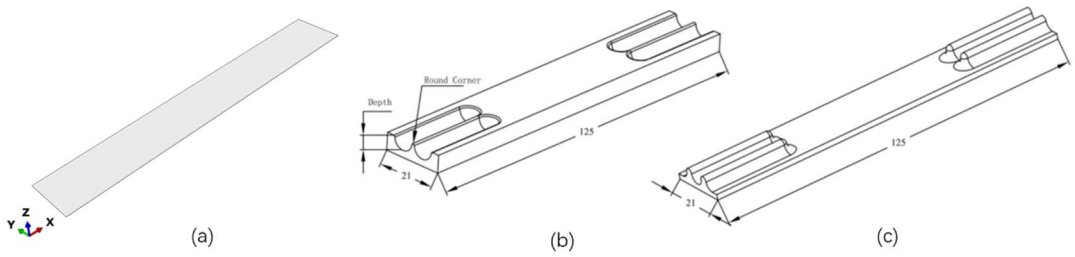

Figure 1. 3D Model

2.2 Creation of Material Properties

The material selected for this paper is 304 stainless steel with a material density of 8e-9 t/mm3, Young's modulus of 194,000 MPa, and Poisson's ratio of 0.28. The material constitutive equation used is the Johnson-Cook constitutive equation with parameters as shown in Table 1.

Table 1. Johnson-Cook Model Parameters[7]

Material	A(MPa)	B(MPa)	n	C	m	T0(°C)	Tm(°C)
SS304	205	1638	0.811	0.014	1	20	1398

2.3 Load Setting and Meshing

A velocity field is predefined and applied to the punch-pin. The punch-pin forms the part at a certain velocity while the cavity mold remains stationary. Figure 2 shows the mesh division, which uses S4R (Four-node linear reduced integration unit) shell unit type with a structural quadrilateral unit shape. The approximate global size is 0.4, and at least five layers of integral units in the thickness direction are guaranteed, totaling 15,650 units. The unit type of the punch-pin and cavity mold is displayed as a discrete rigid body with an approximate global size of 1.0[8]. Seed encryption is applied to the groove and rounded corners to obtain more accurate dimensions of the punch-pin and cavity mold. The total number of units for punch-pin molds is 4,937, and for cavity mold, the total number of units is 5,222. After partitioning the mesh, create the job and verify the data. Submit the job for analysis after confirming that the data is correct.

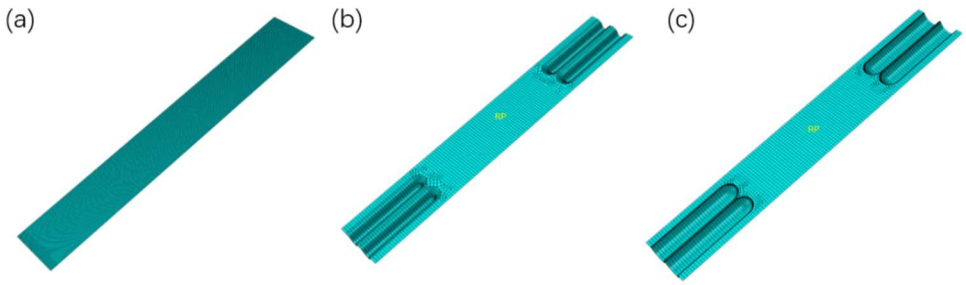

Figure 2. Mesh Division Diagram

ISSN: 2414-1895 DOI: 10.6919/ICJE.202404_10(4).0012

2.4 Process Parameter Setting

The primary process parameters of the stamping process include friction coefficient, stamping speed, groove depth and mold fillet radius[9], which are investigated by using mono factor analysis, and the values of the parameters are shown in Table 2, with the initial values of friction coefficient of 0.08, stamping speed of 2400 mm/s, groove depth of 3.5 mm and mold fillet radius of 0.5 mm.

Table 2. Simulation Parameters

Friction Coefficient	Stamping Speed (mm/s)	Groove Depth (mm)	Mold Fillet Radius (mm)
0.08	1600	3.5	0.3
0.10	2400	3.6	0.4
0.12	3200	3.7	0.5
0.14	4000	3.8	0.6
0.16	4800	3.9	0.7

3. Analysis of Simulation Results for Mono Factor

Mono factor simulation was conducted to study the maximum thinning rate and equivalent plastic strain (PEEQ) after stamping 304 stainless steel. The stamping process allows a maximum thinning rate of 30%. Exceeding this limit can result in an unstable structure. In addition, a larger PEEQ increases the probability of failure and damage[10].

3.1 Analysis of Simulation with Various Friction Coefficients

The analysis involves setting various coefficients of friction. Other parameters include a stamping speed of 2400 mm/s, a groove depth of 3.5 mm, and a mold fillet radius of 3.5 mm. Figure 3 displays the PEEQ and maximum thinning rate for various friction coefficients. The figure shows that both the maximum thinning rate and the PEEQ decrease as the friction coefficient increases from 0.08 to 0.10, but gradually increase from 0.10 to 0.16. The processing effect is better at a friction coefficient of 0.10.

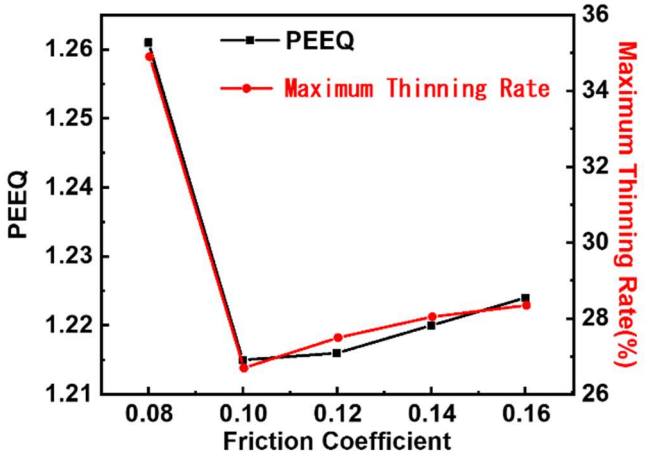

Figure 3. Maximum Thinning Rate and PEEQ for Different Friction Coefficient

3.2 Analysis of Simulation with Various Stamping Speeds

The experimental conditions included a coefficient of friction of 0.10, a groove depth of 3.5 mm, a mold fillet radius of 3.5 mm, and stamping speeds of 1600 mm/s, 2400 mm/s, 3200 mm/s, 4000 mm/s,

ISSN: 2414-1895 DOI: 10.6919/ICJE.202404_10(4).0012

and 4800 mm/s, respectively. Figure 4 displays the maximum thinning rate and PEEQ at various stamping speeds.

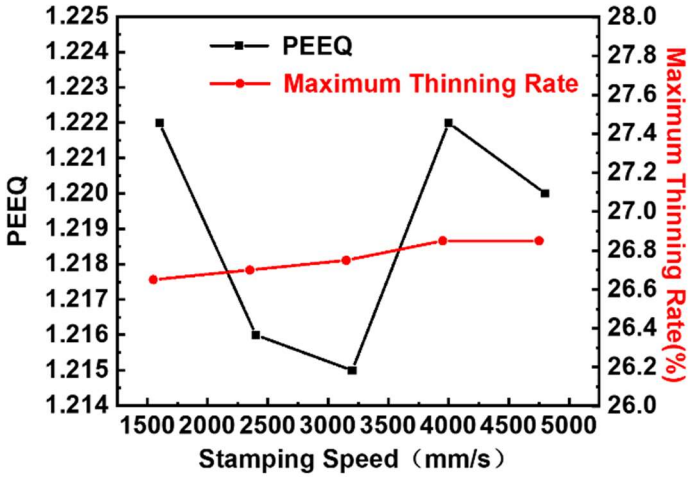

Figure 4. Maximum Thinning Rate and PEEQ for Different Stamping Speed

Figure 4 shows that the maximum thinning rate remains relatively stable between 26.5% and 26.8% as the stamping speed increases. However, the PEEQ changes with the increase in stamping speed, tending to decrease and then increase. The minimum value is obtained at 3200 mm/s, at which point the risk of crack formation is the lowest. In summary, optimal processing is achieved at a stamping speed of 3200 mm/s.

3.3 Analysis of Simulation with Various Groove Depth

Experimental conditions: The friction coefficient is 0.10. The stamping speed is 3200 mm/s. The radius of the mold fillet is 0.5 mm. The depth of the groove is 3.5 mm, 3.6 mm, 3.7 mm, 3.8 mm, and 3.9 mm. Figure 5 displays the plate thickness after forming and the maximum thinning rate and PEEQ.

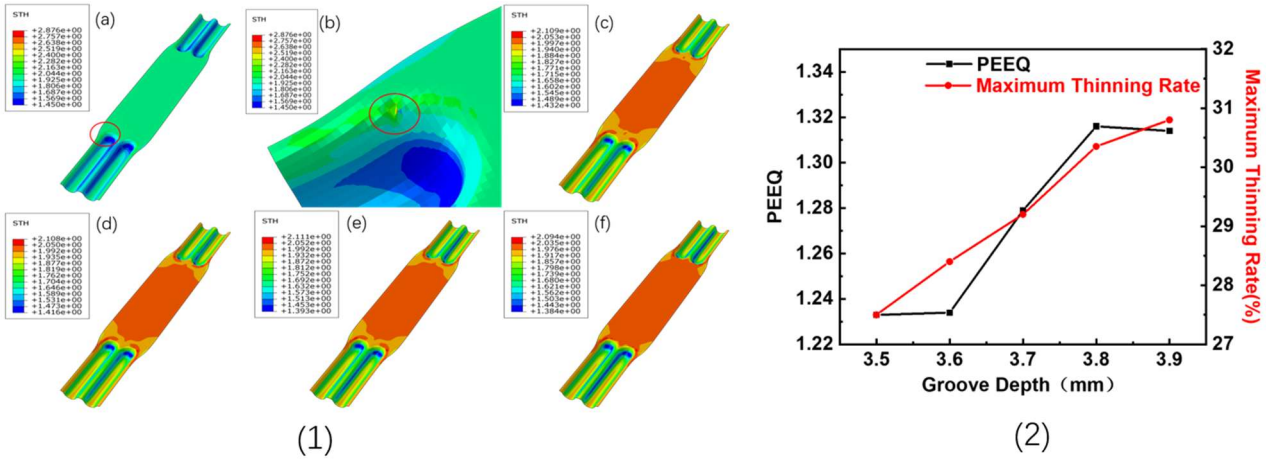

Figure 5. (1) Plate Thickness at Different Groove Depth(a) 3.5 mm; (b) Local Enlargement; (c) 3.6 mm (d) 3.7 mm; (e) 3.8 mm; (f) 3.9 mm; (2) Maximum Thinning Rate and PEEQ for Different Groove Depth

The minimum plate thickness decreases from 1.45 mm to 1.38 mm as the groove depth increases. Due to the lack of plate limitation by the crimping device and the influence of the plate width, a small

ISSN: 2414-1895 DOI: 10.6919/ICJE.202404_10(4).0012

area near the mold fillet of the groove may experience poor material flow, resulting in a plugging condition. In Figure 5 (a) and (b), the maximum plate thickness reaches 2.87 mm and the deformations are uneven. The groove depth continues to increase, the maximum plate thickness gradually decreases, and the maximum thinning rate increases. When the depth of the groove reaches 3.8 mm, the maximum thinning rate reaches 30.35%, which exceeds the safe range. Under the given process conditions and structural design, a groove depth of 3.7 mm is more appropriate, and the maximum thinning rate is 29.20%, which is within the safe range.

3.4 Analysis of Simulation with Various Mold Fillet Radius

The friction coefficient is set to be 0.10, the stamping speed is 3200 mm/s, the depth of the groove is 3.7 mm, and the radius of the mold fillet is 0.3 mm, 0.4 mm, 0.5 mm, 0.6 mm, and 0.7 mm, respectively. Figure 6 shows the maximum thinning rate and PEEQ with different radius of the mold fillet.

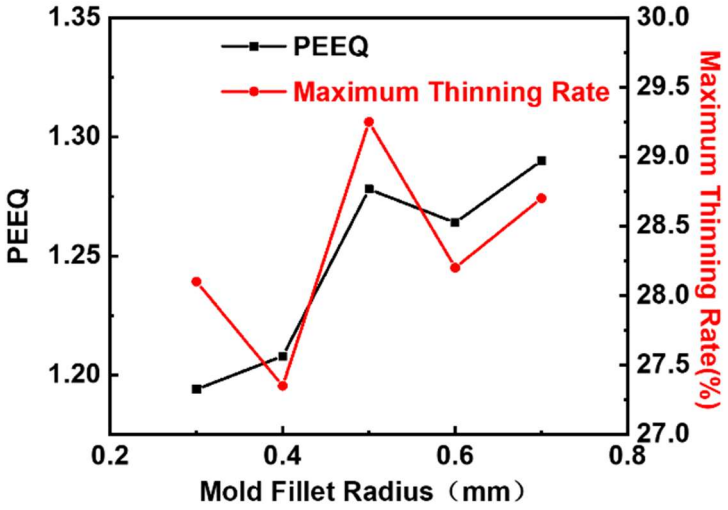

Figure 6. Maximum Thinning Rate and PEEQ for Different Mold Fillet Radius

In Figure 6, the maximum thinning rate after molding with various mold fillet radius and PEEQ is shown. The graph illustrates that the maximum thinning of the plate varies as the radius of the fillet changes from 0.3 mm to 0.5 mm. Specifically, the maximum thinning initially decreases, then increases, and reaches its minimum value when the radius of the fillet is 0.5 mm before increasing and then decreasing again. The maximum thinning rate is at its minimum when the fillet radius is 0.4mm, at a value of 27.35%.

The PEEQ's maximum value is concentrated near the fillet of the groove and increases gradually as the fillet radius increases from 0.3 mm to 0.4 mm. The PEEQ increases significantly as the fillet radius continues to increase up to 0.5 mm, followed by a slow decrease, and then continues to increase, reaching a maximum at 0.7 mm. In summary, optimal processing results are achieved with a mold fillet radius of 0.4 mm.

4. Orthogonal Test Design for Stamping and Forming

4.1 Orthogonal Test Indicators

In both simulation and actual machining, the maximum thinning rate is a crucial indicator of molding quality. It is unsafe to use, even if no damage occurs during processing, if the maximum thinning rate exceeds the allowable limit. Therefore, the experimental index was selected as the maximum thinning rate[11].

ISSN: 2414-1895 DOI: 10.6919/ICJE.202404_10(4).0012

4.2 Factors and Levels Design

The selection of factors and levels is the focus of orthogonality tests[12]. The following factors were selected based on the results of the mono factor test: (A) Friction Coefficient, (B) Stamping Speed, (C) Depth of Groove, (D) Mold Fillet Radius. There were 16 sets of trials, each with four levels for every factor. As shown in Table 3.

Table 3. Factors and Levels of Orthogonal Test

Friction Coefficient	Stamping Speed (mm/s)	Groove Depth (mm)	Mold Fillet Radius (mm)
0.10	2400	3.6	0.4
0.12	3200	3.7	0.5
0.14	4000	3.8	0.6
0.16	4800	3.9	0.7

Table 4. Factors and Levels of Orthogonal Test

Test No.	Factor A	Factor B	Factor C	Factor D	Indicators
	Stamping Speed(mm/s)	Friction Coefficient	Mold Fillet Radius (mm)	Depth of Groove(mm)	Maximum Thinning Rate(%)
Test 1	2400	0.05	0.4	3.6	31.60
Test 2	2400	0.10	0.6	3.7	28.45
Test 3	2400	0.15	0.8	3.8	29.40
Test 4	2400	0.20	1.0	3.9	32.80
Test 5	2800	0.05	0.6	3.8	29.60
Test 6	2800	0.10	0.4	3.9	29.45
Test 7	2800	0.15	1.0	3.6	29.25
Test 8	2800	0.20	0.8	3.7	30.80
Test 9	3200	0.05	0.8	3.9	29.10
Test 10	3200	0.10	1.0	3.8	29.70
Test 11	3200	0.15	0.4	3.7	29.10
Test 12	3200	0.20	0.6	3.6	29.60
Test 13	3600	0.05	1.0	3.7	28.95
Test 14	3600	0.10	0.8	3.6	28.40
Test 15	3600	0.15	0.6	3.9	30.50
Test 16	3600	0.20	0.4	3.8	30.75

ISSN: 2414-1895 DOI: 10.6919/ICJE.202404_10(4).0012

The speed of stamping falls within the range of 2400~3600 mm/s. To minimize PEEQ, the range is narrowed down to smaller values within this interval. The coefficient of friction was measured over a wider range, from 0.05 to 0.20. The fillet radius maximum value has been increased to 1.0 mm.

4.3 Range Analysis

Table 5. Range Analysis

Level	Stamping Speed (mm/s)	Friction Coefficient	Mold Fillet Radius (mm)	Depth of Groove (mm)
K_1	122.25	119.25	120.90	118.85
K_2	119.10	116.00	118.15	117.30
K_3	117.50	118.25	117.70	119.45
K_4	118.60	123.95	120.70	121.85
k_1	30.56	29.81	30.23	29.71
k_2	29.77	29.00	29.54	29.32
k_3	29.38	29.56	29.43	29.86
k_4	29.65	30.99	30.18	30.46
R	1.19	1.99	0.80	1.14
Factor Priority	B>A>D>C			
Excellent Level	A3	B2	C3	D2
Optimal Solution	$B_2A_3D_2C_3$			

Using the maximum thinning rate as an indicator of the stamping and forming performance of conveyor belt buckles, the degree of influence of each process parameter is as follows: Friction Coefficient>Stamping Speed>Depth of Groove>Mold Fillet Radius, as shown in Table 5. The optimal combination of process parameters was determined through range analysis, resulting in B2A3D2C3.The maximum thinning rate is minimized when the stamping speed is 3200 mm/s, the groove depth is 3.7 mm, and the mold fillet radius is 0.8 mm.

4.4 Validation of Optimized Process Parameters

Using the optimal stamping process parameters again for 304 stainless steel conveyor belt buckle grooves stamping and forming verification, the maximum thinning rate obtained is 27.50%, and distributed in the groove near the large round corner. The simulation results for the optimal process parameters were compared to the results of the 16 sets of orthogonal tests that were designed. The optimized process parameters minimize the maximum thinning rate, demonstrating the correctness and rationality of the orthogonal test design. It also provides guidance for stamping and forming of 304 stainless steel conveyor belt buckles.

5. Conclusion

Mono factor analysis was conducted on the four main parameters for stamping and forming 304 stainless steel conveyor belt buckle grooves. These parameters include friction coefficient, stamping speed, mold fillet radius, and groove depth. The study aimed to investigate their effects on the maximum thinning rate and PEEQ. The simulation results were analyzed to determine the range of optimal process parameters for stamping and forming. The mono factor analysis has selected the following optimal parameters: friction coefficient of 0.10, stamping speed of 3200 mm/s, mold fillet radius of 0.4 mm, and groove depth of 3.7 mm. This study conducted a single-factor analysis to

ISSN: 2414-1895 DOI: 10.6919/ICJE.202404_10(4).0012

determine the maximum thinning rate of plate stamping. The stamping gap was set to 2.10 mm, and four levels were selected for the remaining four process parameters. A total of 16 groups were designed for the four orthogonal tests with four factors and four levels. The maximum thinning rate was obtained for each factor level, and the results were analyzed using range analysis. The analysis results indicate that the optimal process parameters are: stamping speed of 3200 mm/s, friction coefficient of 0.10, mold radius of 0.8 mm, and groove depth of 3.7 mm. Simulation using these parameters resulted in a maximum thinning rate of 27.50%, which is smaller than the results of the 16 groups of orthogonal experiments. This confirms the accuracy of the orthogonal experiments and provides guidance for practical machining processes.

References

[1] Zhang M, Sun N, Zhang Y, et al. A centernet-based direct detection method for mining conveyer belt damage[J]. Journal of Ambient Intelligence and Humanized Computing, 2023, 14(4): 4477-4487.

[2] Su Y, Zhao G, Zhao Y, et al. Multi-Objective Optimization of Cutting Parameters in Turning AISI 304 Austenitic Stainless Steel[J]. Metals, 2020, 10(2).

[3] Andrejiova M, Grincova A, Marasova D. Measurement and simulation of impact wear damage to industrial conveyor belts[J]. Wear, 2016, 368: 400-407.

[4] Lan X, Hu B, Cheng H, et al. Quantitative study on the effect of stress magnetization of martensite in 304 austenitic stainless steel[J]. Engineering Failure Analysis, 2022, 138: 106390.

[5] Li G, Long X, Yang P, et al. Advance on friction of stamping forming[J]. The International Journal of Advanced Manufacturing Technology, 2018, 96: 21-38.

[6] Mori K-I, Nonaka T. Simplified three-dimensional finite element simulation of shear spinning process based on axisymmetric modeling[J]. Journal of manufacturing processes, 2005, 7(1): 51-56.

[7] Korkmaz H G, Toros S, Halkaci M, et al. Investigation of hydro-piercing method for stainless steels by finite element method[C]. MATEC Web of Conferences, 2018: 01003.

[8] Yu G, Zhao J, Wang C, et al. Development of a cold stamping process for forming single-welded elbows[J]. The International Journal of Advanced Manufacturing Technology, 2017, 88: 1911-1921.

[9] Jiang B, Huang J, Ma H, et al. Multi-Objective Optimization of Process Parameters in 6016 Aluminum Alloy Hot Stamping Using Taguchi-Grey Relational Analysis[J]. Materials, 2022, 15(23): 8350.

[10] Zheng J, Shu X, Wu Y, et al. Investigation on the plastic deformation during the stamping of ellipsoidal heads for pressure vessels[J]. Thin-Walled Structures, 2018, 127: 135-144.

[11] Thu N T, Trung N D. On the thickness distribution and the maximum thinning ratio in hydrostatic forming for sheet metal[J]. International Journal of Modern Physics B, 2020, 34(22n24): 2040144.

[12] Liu J, Wang Q-B, Zhao H-T, et al. Optimization design of the stratospheric airship's power system based on the methodology of orthogonal experiment[J]. Journal of Zhejiang University-Science A, 2013, 14(1): 38-46.